Mem. S.A.It. Suppl. Vol. 14, 78

Memorie della
Supplementi

The dusty Universe: astronomy at infrared wavelengths

L. K. Hunt

Istituto Nazionale di Astrofisica – Osservatorio Astrofisico di Arcetri, Largo Enrico Fermi 5, I-50125 Firenze, Italy, e-mail: hunt@arcetri.astro.it

Abstract. The last twenty years have shown ever more convincingly that most of the star formation activity in the universe is enshrouded in dust. Half of the energy and most of the photons pervading intergalactic space come from the infrared (IR) spectral region. In this review, I describe briefly what has been discovered with *IRAS*, *ISO*, and now *Spitzer*, and look ahead toward the recently launched IR satellite, *Herschel*, and the future *JWST*. The focus is extragalactic, mainly star-forming galaxies, and on diagnostics to distinguish them from galaxies hosting active nuclei. I will illustrate the importance of IR wavelengths for probing dust-enshrouded starbursts, quantifying physical processes in the interstellar medium, and measuring star-formation density across cosmic time. Particular attention will be paid to trends with metal abundance; studying how stars form in nearby metal-poor galaxies can help understand the transition between primordial star formation in metal-free environments and the chemically evolved starbursts in the Local Universe.

Key words. Infrared: galaxies – Galaxies: ISM – Galaxies: starburst – Galaxies: evolution – galaxies: formation Cosmology: observations

1. Introduction

First *IRAS* and *ISO*, and more recently SCUBA, *COBE*, and *Spitzer* have convincingly shown that most of the star formation in the universe is obscured. Populations of infrared-luminous galaxies at $z \lesssim 1.5$ constitute about 70-80% of the far-infrared and 30% of the sub-millimeter backgrounds, respectively, and probably dominate the star-formation activity at high redshift (e.g., Chary & Elbaz 2001; Le Floc'h et al. 2005; Dole et al. 2006), Indeed, half the energy and most of the photons in the universe come from the infrared spectral region (e.g., Hauser & Dwek 2001; Franceschini et al. 2008).

That dust is so prominent in the high-redshift universe may appear surprising, since dust would be expected to not exist in the absence of metals. However, recent theoretical developments belie the assumption that dust is absent at low metallicity; conspicuous amounts of dust can be created on short timescales by supernovae (SNe) and Asymptotic Giant Branch stars which evolve in a metal-free ISM (e.g., Todini & Ferrara 2001; Bianchi & Schneider 2007; Valiante et al. 2009). Copious dust emission is indeed observed at very high redshifts ($z \gtrsim 6$) in quasars (Bertoldi et al. 2003), with the implication that dust formation can

Send offprint requests to: L. Hunt

be very rapid at early times as proposed theoretically. Although luminous quasars can hardly be considered typical examples of star-formation processes, the properties of sub-millimeter galaxies (SMGs, Chapman et al. 2005) and dust-obscured galaxy populations (DOGs, Dey et al. 2008) also suggest that star formation episodes can be very intense, enshrouded in dust, and relatively brief. However, exactly how these massive dusty starbursts occur and evolve is not yet clear. The short interval in which star formation and the ensuing chemical enrichment and dust formation convert a dust-free metal-free environment to a dusty metal-rich one at high redshift is as yet unobserved, and remains a major observational challenge.

2. Dust and star formation

IRAS identified a new infrared (IR) galaxy population, the Luminous Infrared Galaxies (LIRGs) with luminosities $L_{FIR} \sim 10^{10} - 10^{12}\,L_\odot$ (Soifer et al. 1987). The most extreme cases with $L_{FIR} \gtrsim 10^{12}\,L_\odot$ were termed ULIRGs, Ultraluminous IR galaxies. Dust obscuration, as quantified by the ratio of IR to *B*-band luminosity, L_{FIR}/L_B, was found to depend significantly on luminosity, with the most luminous sources also being the most obscured. Figure 1 shows spectral energy distributions (SEDs) taken from the very successful GRASIL models by the group at Padova (Silva et al. 1998). The remarkable IR SED in Arp 220 (see Fig. 1) was discovered by *IRAS*; this galaxy is one of several prototypical ULIRGs in the Local Universe. It is evident that as galaxies harbor more star formation, their dust opacity increases; indeed, in galaxies with IR-dominated SEDs, such as M 82 and Arp 220, the SFR is quite well correlated with L_{FIR}, making L_{FIR} a powerful SFR tracer (Kennicutt 1998). In this case, L_{FIR} is a very good predictor of bolometric luminosity, because dust reprocesses virtually all of the ultraviolet radiation emitted at shorter wavelengths.

2.1. LIRGs, ULIRGs, and SMGs

Apart from their high dust opacity, perhaps the most noteworthy characteristic of LIRGs and ULIRGs is their high SFR per unit area. Optically such galaxies are quite nondescript, since dust patches hide most of the "action"; however, the obscuring dust emits so strongly at IR wavelengths that it dominates the SED, making the IR the only realistic spectral regime to study the energetics of the star formation. The power behind the IR luminosity is almost inevitably mergers or interactions of gas-rich spiral galaxies. In the case of Arp 220, 95% of the light is produced by the interaction; the core, ∼1 kpc in diameter, contains 200 star clusters and as much molecular gas as the entire Milky Way, $M_{H2} \sim 10^8 M_\odot$ (Scoville et al. 1998; Wilson et al. 2006). This means that the gas surface density is $\sim 6 \times 10^4 M_\odot\,pc^{-2}$, about 20 times that in the LIRG, M 82, a prototypical IR starburst. Furthermore, the SFR density is $\sim 10^3 M_\odot\,yr^{-1}\,kpc^{-2}$, more than 10 times higher than the maximum-intensity starburst limit predicted by Meurer et al. (1997).

About 30% of the ULIRG population harbor active galactic nuclei (AGN) (Genzel et al. 1998). The frequency of this occurrence is a strong function of luminosity; about half the ULIRGs with $L_{FIR} \gtrsim 2 \times 10^{12}\,L_\odot$ contain AGN, below this luminosity, only about 15% of them do (Lutz et al. 1998). Nevertheless, most of the IR (thus bolometric) luminosity in ULIRGs comes from star formation; only in hard X rays does an unambiguous AGN signature emerge (Gerssen et al. 2004; Polletta et al. 2006).

SMGs, discovered ∼10 years ago through their strong 850 μm continuum (e.g., Hughes et al. 1998), are very dusty, very luminous galaxies at redshifts $z \sim 2 - 3$, with cooler dust than ULIRGs (Pope et al. 2006). SMGs tend to be more gas rich than local ULIRGs, with ∼20–50% of their mass in gas (Tacconi et al. 2006, 2008). They are also quite compact and dense, compared with other (optically bright) galaxies at $z \sim 2$ (Bouché et al. 2007). In fact, their SEDs, broader than those of ULIRGs, are better approximated by models of dusty, compact, dense star clusters than by LIRG and ULIRG templates

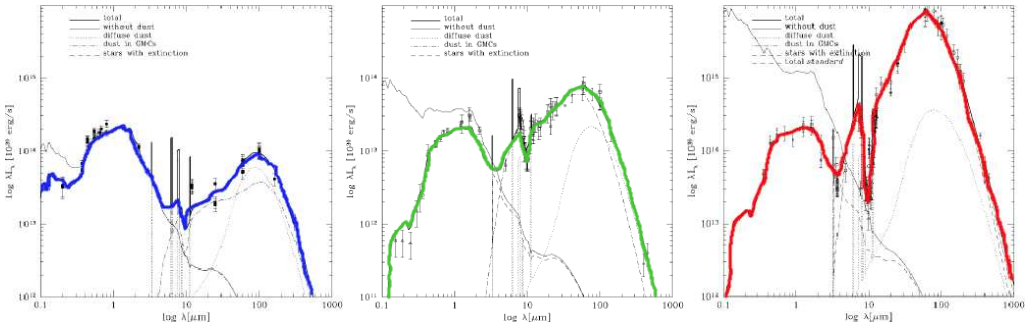

Fig. 1. SEDs of three representative galaxies taken from Silva et al. (1998), shown from left to right (M 100, M 82, Arp 220) as a function of increasing dust opacity, luminosity, and SFR.

(Hunt & Maiolino 2005). The small sizes and large matter densities of SMGs imply that they, like ULIRGs, host high-intensity starbursts, forming stars at a rate an order of magnitude greater than UV/optically-selected galaxies of similar dynamical mass (Bouché et al. 2007).

3. The interstellar medium

Spectral lines and features in the IR regime constitute the most important coolants for the ISM. Fine structure (FS) spectral lines such as [Si II] (35 μm), [O I] (63 μm), and [C II] (158 μm) can emit more than 0.1% of the bolometric luminosity of a star-forming galaxy and are the dominant cooling lines for neutral ISM gas in Photo-Dissociated Regions (PDRs). Other lines, such as [Ne II] (12.8 μm), [Ne III] (15.6 μm), [S III] (18, 33 μm), [O III] (52, 88 μm), and [N II] (122, 205 μm) are strong coolants for ionized gas in H II regions.

Molecular emission in the form of H_2O, OH, and rotational transitions of H_2 are important IR tracers of warm neutral gas in the ISM. These molecules, which emit in the range of ~10 to 200 μm constrain gas density and temperature, and help quantify how stars form under different physical conditions in the ISM.

Finally, dust spectral emission features, usually identified with Polycyclic Aromatic Hydrocarbons (PAHs), dominate the mid-infrared spectrum of most star-forming galaxies. They are broad features, sometimes blended, with the strongest ones peaking at 3.3, 6.2, 7.7, 8.6, 11.2, and 12.6 μm. Discovered by *IRAS*, and probed in detail by the spectrometers on board *ISO*, PAHs can emit as much as ~ 10 – 20% of the IR energy budget (Brandl et al. 2006; Smith et al. 2007). Through the photoelectric effect, PAHs heat the gas in the ISM (e.g., Hollenbach & Tielens 1997), thereby reinforcing the coupling of the gas and dust components. Because they are so dominant in the mid-infrared (MIR) spectral range, PAHs have been used to identify galaxies with intense star formation at redshifts of ~ 2 – 3 (see Sect. 4), and to estimate their bolometric luminosities (e.g., Houck et al. 2007; Weedman & Houck 2008; Dey et al. 2008).

3.1. The ISM at low metallicity

ISO and *Spitzer* have dispelled the "myth" that dust is absent in a metal-poor ISM; dust can be abundant and the infrared spectra of low-metallicity star-forming dwarf galaxies show a variety of shapes (e.g., Madden et al. 2006; Wu et al. 2006). Cooling is less efficient in a metal-poor ISM, so hardness and intensity of the interstellar radiation field (ISRF) increases. Flux ratios of high-ionization species can be adopted to infer the ISRF hardness, or equivalently the UV slope of its spectrum, which is sensitive to the effective temperatures of the ionizing stars. In the IR range, the flux ratios of [Ne III]/[Ne II] (ionization potentials of 41 and 21.6 eV, respectively) and [S IV]/[S III] (34.8 and23.3 eV, respectively) are usually used (e.g., Thornley et al. 2000; Giveon et al. 2002). Figure 2 shows the ratio of

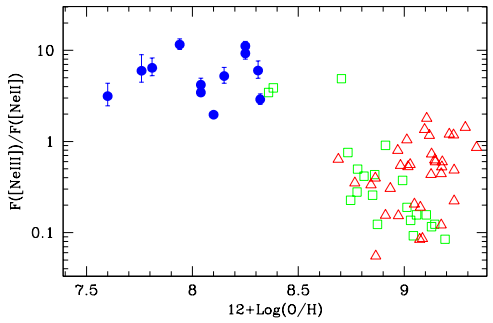

Fig. 2. [Ne III]/[Ne II] ratios plotted against the nebular oxygen abundance, 12+log(O/H). Low-metallicity galaxies are shown as filled circles, while the SINGS galaxies (Dale et al. 2009) as open squares (H II region-nuclei) and open triangles (AGN) (taken from Hunt et al. 2009).

[Ne III] to [Ne II] plotted against oxygen abundance for a sample of metal-rich star-forming galaxies (the SINGS sample: Kennicutt et al. 2003; Dale et al. 2009) and low-metallicity star-forming dwarf galaxies (Hunt et al. 2009). The [Ne III]/[Ne II] ratio increases by almost a factor of ∼10 over a decade of metallicity. The hardness of the ISRF at low metal abundance can approach or exceed that in AGN (see Sect. 3.2). However, the scatter of the [Ne III]/[Ne II] flux ratio at a given oxygen abundance is large, indicating that metallicity cannot be the only parameter controlling the hardness of the ISRF.

The ISRF hardness and intensity govern dust properties such as the grain size distribution and temperature. In most star-forming galaxies, PAH emission shows a surprisingly narrow range of properties, and can be well characterized by a "standard set" of features with well-defined wavelengths and FWHMs (Smith et al. 2007). However, first *ISO* and later *Spitzer* have shown that metal-poor star-forming galaxies and AGN are deficient in PAH emission (Madden et al. 2006; Wu et al. 2006; Hunt et al. 2009). It is likely that the hard and intense ISRFs at low metallicity and in AGN destroy the PAHs typical of metal-rich star-forming galaxies (e.g., Voit 1992; Madden et al. 2006; Smith et al. 2007). The PAH emission in metal-poor star-forming galaxies is, on average, ∼8 times lower than in metal-rich ones (1.3% vs. 10% when normalized to L_{FIR}, Hunt et al. 2009).

3.2. AGN/starburst diagnostics

While PAH features are strong in metal-rich star-forming galaxies, they are deficient in low-metallicity galaxies and in AGN. In fact, a deficit of PAH emission, combined with FS line indicators of excitation, has often been used as a AGN diagnostic in solar metallicity star-forming galaxies. Genzel et al. (1998) proposed the ratio of [O IV] and [Ne II] compared to the strength of the strongest PAH feature at 7.7 μm. [O IV] (25.9 μm) has an ionization potential of 54.9 eV, compared to 21.6 eV for [Ne II], so traces the same ISRF hardness as needed to ionize helium. Figure 3 shows such a diagram for ULIRGs, metal-rich starbursts, and low-metallicity star-forming dwarf galaxies. For metal-rich systems, plotting these two ratios against one another results in a clear distinction between star-forming galaxies (stars and squares) and AGN (triangles), the latter having a higher [O IV]/[Ne II] ratio and a weaker 7.7 μm PAH feature than the former. However, the situation for low-metallicity galaxies is different; because of their hard ISRF, half the metal-poor star-forming galaxies in Fig. 3 would have been classified as pure AGN. Thus, at low metallicity, the [O IV]/[Ne II] vs. 7.7 μm PAH band diagnostic does not distinguish starbursts from AGN.

A second AGN diagnostic (Laurent et al. 2000) exploits the steeply rising MIR continuum in starbursts, compared to the flatter continua in AGN and quiescent star-forming regions (or PDRs). Most star-forming galaxies have both PDR and H II region components in their spectra; the PDR component tends to have a flat MIR continuum and be dominated by PAH bands, while the H II regions have a deficiency of PAHs and a steeply rising MIR continuum from warm dust. Because of their steep MIR continua, similar to H II regions, low-metallicity dwarf galaxies are clearly distinguished from the AGN, ULIRGs, and metal-rich star-forming galaxies, the latter more similar to PDRs because of their strong PAH com-

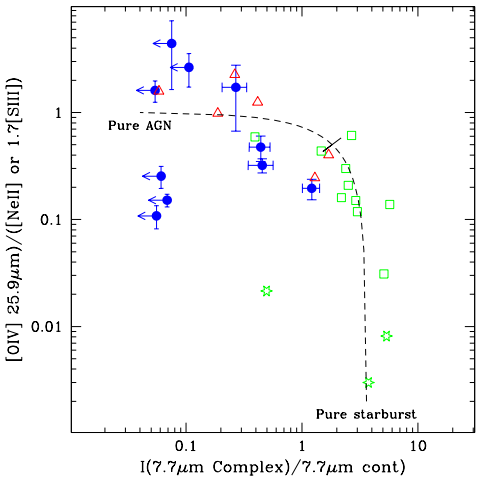

Fig. 3. [O IV][Ne II] vs. the strength of the 7.7 μm PAH feature. The data for starburst galaxies, ULIRGs, and AGN are marked by stars, open squares, and open triangles, respectively (taken from Genzel et al. 1998); low-metallicity objects are denoted by filled circles (taken from Hunt et al. 2009).

ponent. This AGN/starburst diagnostic effectively separates AGN from starbursts, even in the low metallicity regime.

A third method for identifying AGN in LIRGs and ULIRGs has been developed more recently by Risaliti and collaborators, and exploits the 3.3 μm PAH strength compared to the 3-4 continuum slope. Obscured AGN always have steeper slopes than starbursts, because of more hot dust, and lower PAH equivalent widths (Risaliti et al. 2006). This technique has been extended to molecular absorption features in the 4-5 μm range, and to longer wavelength PAHs observed by *Spitzer* (Sani et al. 2008; Nardini et al. 2008).

4. An infrared census of the high-redshift universe

Because the most prominent PAH features at 7-8 μm are redshifted into the *Spitzer*/MIPS 24 μm band for z ~2, selecting objects in deep fields with 24 μm detections and very faint optically has revealed new IR galaxy populations. One of these, the DOGs, are ULIRG-like with warmer dust than SMGs, and may represent, like ULIRGs, an AGN-growth phase in galaxy evolution. Another population at z ~2-3, obscured Compton-thick AGN (Fiore et al. 2008), has been found by selecting sources in deep fields with very red colors ($R - K > 5$) and 24 μm detections. Other selection techniques include the redshifted stellar photospheric bump (rest-frame 1.6 μm) and requiring 70 μm detections with *Spitzer* (Farrah et al. 2008; Brand et al. 2008). All these criteria select IR-luminous galaxy populations qround $z \sim 2$, and are able to sample luminosities $\gtrsim 10^{11} L_{\odot}$.

By comparing bolometric luminosities to those derived in the IR and the UV, it is possible to infer obscuration as a function of redshift and luminosity. This has been done by Reddy et al. (2006) using MIPS 24 μm fluxes in GOODS fields to estimate restframe 5-8 μm (PAH) luminosities for galaxies at z ~2, and comparing these with local and other high z samples. Results show that obscuration increases dramatically with luminosity, and that the fraction of star-formation episodes occurring in dust-obscured systems increases with redshift. However, for a given bolometric luminosity, the obscuration at z ~2 is lower than locally by almost an order of magnitude. This means that dust obscuration has less of an impact on high-z galaxy observations than would be expected from present-day extrapolation.

5. Future perspectives

With *Spitzer*, galaxy populations of luminosities $\gtrsim 10^{11} L_{\odot}$. can be sampled to $z \sim 2$, but with *Herschel* such luminosities will be routinely sampled to $z \sim 3$. Such sensitivity has immense discovery potential, and *Herschel* continuum surveys from 100 to 500 μm will be able to constrain bolometric luminosity, cold-dust masses, and identify AGN populations beyond epochs currently possible in the far-IR. On the other hand, at short-IR wavelengths up to ~25 μm, *JWST* should increase sensitivity relative to *Spitzer*/IRAC by a factor of 10 or so, making it possible to probe galaxy ages and masses toward the epoch of reionization.

Acknowledgements. I am grateful to the organizers for the invitation to give this review on infrared astronomy.

References

Bianchi, S., & Schneider, R. 2007, MNRAS, 378, 973
Bertoldi, F., Carilli, C. L., Cox, P., Fan, X., Strauss, M. A., Beelen, A., Omont, A., & Zylka, R. 2003, A&A, 406, L55
Bouché, N., et al. 2007, ApJ, 671, 303
Brand, K., et al. 2008, ApJ, 673, 119
Brandl, B. R., et al. 2006, ApJ, 653, 1129
Chapman, S. C., Blain, A. W., Smail, I., & Ivison, R. J. 2005, ApJ, 622, 772
Chary, R., & Elbaz, D. 2001, ApJ, 556, 562
Dale, D. A., et al. 2009, ApJ, 693, 1821
Dey, A., et al. 2008, ApJ, 677, 943
Dole, H., et al. 2006, A&A, 451, 417
Farrah, D., et al. 2008, ApJ, 677, 957
Fiore, F., et al. 2008, ApJ, 672, 94
Franceschini, A., Rodighiero, G., & Vaccari, M. 2008, A&A, 487, 837
Genzel, R., et al. 1998, ApJ, 498, 579
Gerssen, J., van der Marel, R. P., Axon, D., Mihos, J. C., Hernquist, L., & Barnes, J. E. 2004, AJ, 127, 75
Giveon, U., Sternberg, A., Lutz, D., Feuchtgruber, H., & Pauldrach, A. W. A. 2002, ApJ, 566, 880
Hauser, M. G., & Dwek, E. 2001, ARA&A, 39, 249
Hollenbach, D. J., & Tielens, A. G. G. M. 1997, ARA&A, 35, 179
Houck, J. R., Weedman, D. W., Le Floc'h, E., & Hao, L. 2007, ApJ, 671, 323
Hughes, D. H., et al. 1998, Nature, 394, 241
Hunt, L. K., & Maiolino, R. 2005, ApJ, 626, L15
Hunt, L. K., Thuan, T. X., Izotov, Y. I., & Sauvage, M. 2009, ApJ, submitted
Kennicutt, R. C., Jr. 1998, ARA&A, 36, 189
Kennicutt, R. C., Jr., et al. 2003, PASP, 115, 928
Laurent, O., Mirabel, I. F., Charmandaris, V., Gallais, P., Madden, S. C., Sauvage, M., Vigroux, L., & Cesarsky, C. 2000, A&A, 359, 887
Le Floc'h, E., et al. 2005, ApJ, 632, 169
Lutz, D., Spoon, H. W. W., Rigopoulou, D., Moorwood, A. F. M., & Genzel, R. 1998, ApJ, 505, L103
Madden, S. C., Galliano, F., Jones, A. P., & Sauvage, M. 2006, A&A, 446, 877
Meurer, G. R., Heckman, T. M., Lehnert, M. D., Leitherer, C., & Lowenthal, J. 1997, AJ, 114, 54
Nardini, E., Risaliti, G., Salvati, M., Sani, E., Imanishi, M., Marconi, A., & Maiolino, R. 2008, MNRAS, 385, L130
Peeters, E., Spoon, H. W. W., & Tielens, A. G. G. M. 2004, ApJ, 613, 986
Polletta, M. d. C., et al. 2006, ApJ, 642, 673
Pope, A., et al. 2006, MNRAS, 370, 1185
Reddy, N. A., Steidel, C. C., Fadda, D., Yan, L., Pettini, M., Shapley, A. E., Erb, D. K., & Adelberger, K. L. 2006, ApJ, 644, 792
Risaliti, G., et al. 2006, MNRAS, 365, 303
Sani, E., et al. 2008, ApJ, 675, 96
Scoville, N. Z., et al. 1998, ApJ, 492, L107
Silva, L., Granato, G. L., Bressan, A., & Danese, L. 1998, ApJ, 509, 103
Smith, J. D. T., et al. 2007, ApJ, 656, 770
Soifer, B. T., Neugebauer, G., & Houck, J. R. 1987, ARA&A, 25, 187
Tacconi, L. J., et al. 2006, ApJ, 640, 228
Tacconi, L. J., et al. 2008, ApJ, 680, 246
Thornley, M. D., Schreiber, N. M. F., Lutz, D., Genzel, R., Spoon, H. W. W., Kunze, D., & Sternberg, A. 2000, ApJ, 539, 641
Todini, P., & Ferrara, A. 2001, MNRAS, 325, 726
Valiante, R., Schneider, R., Bianchi, S., & Andersen, A. C. 2009, MNRAS, 397, 1661
Voit, G. M. 1992, MNRAS, 258, 841
Weedman, D. W., & Houck, J. R. 2008, ApJ, 686, 127
Wilson, C. D., Harris, W. E., Longden, R., & Scoville, N. Z. 2006, ApJ, 641, 763
Wu, Y., Charmandaris, V., Hao, L., Brandl, B. R., Bernard-Salas, J., Spoon, H. W. W., & Houck, J. R. 2006, ApJ, 639, 157